BROOKHAVEN
NATIONAL LABORATORY

BNL-79837-2008-CP

Transport and Magnetization Properties of Rolled RRP Nb_3Sn Strands

A.K. Ghosh, L.D. Cooley, D.R. Dietderich and L. Sun

Presented at
20th International Conference on Magnet Technology
Philadelphia, PA
August 27-31, 2007

January 29, 2008

Superconducting Magnet Division

Brookhaven National Laboratory
P.O. Box 5000
Upton, NY 11973-5000
www.bnl.gov

DISCLAIMER

Transport and Magnetization Properties of Rolled RRP Nb_3Sn Strands

A. K. Ghosh, L. D. Cooley, D. R. Dietderich and L. Sun

Abstract—**Restack Rod Process (RRP) strands with 54 and 108 sub-elements were rolled from 0.7 mm diameter to 0.45 mm thickness to simulate the deformation of strands at the edges of Rutherford cables. Various diagnoses were then applied to assess performance and stability. Transport measurements were used to assess the effect of rolling on the critical current. Magnetization measurements were used to probe superconducting pathway bridging between deformed sub-elements. The copper residual resistivity ratio *RRR* was also measured to assess tin contamination due to thinned or ruptured diffusion barriers. While systematic changes were observed in all three measurements with increasing deformation, *RRR* showed the strongest changes. The implications of these measurements for cable stability, and their relationship to observations of the strand cross-section by light microscopy, are discussed.**

Index Terms—**Niobium-Tin compounds, electric property measurements, cabling degradation, magnetic property measurements.**

I. Introduction

High field magnets being developed for particle accelerators beyond the Large Hadron Collider (LHC) use superconducting wires with high critical current density J_c based on the compound Nb_3Sn. Rutherford cables [1] made from Nb_3Sn wires are being used in the LHC Accelerator Research Program (LARP) to develop quadrupole magnets with high gradients exceeding 200 T m^{-1}. Such magnets could be used in a future luminosity upgrade of the LHC by replacing the interaction region Nb-Ti quadrupoles with Nb_3Sn quadrupoles operating at 12-16 T.

The present state of Nb_3Sn wire art provides high J_c, e.g. >3000 A·mm^{-2} in the non-copper region at 12 T and 4.2 K. This performance benchmark has routinely been achieved by Oxford Instruments, Superconducting Technology (OST) in Restack-Rod-Process (RRP) strands [2]. Sub-elements consisting of ~1,000 Nb alloy filaments in a copper matrix are restacked around a central Sn-alloy core in this process. During reaction, the small Nb filaments expand upon conversion to Nb_3Sn and merge together, forming a continuous superconducting region with an effective diameter equal to that of the entire sub-element. Such large filaments (henceforth, filament is used synonymously with sub-element) are not stable against flux jumps. Moreover, each sub-element is surrounded by a Nb barrier, and in fact, the barrier is intentionally reacted part-way through to maximize the Nb_3Sn fraction and thereby maximize the non-copper J_c. Because there is the potential for tin to diffuse completely through thin regions of the barrier and into the stabilizing copper, poor thermal conductivity of the stabilizer can exacerbate the poor stability against flux-jumps. Past work demonstrates the correlation between copper residual resistivity ratio *RRR* and a stability threshold current density, J_s, above which heat released by low-field flux jumps results in a temperature rise that cannot be recovered [3].

RRP and other internal-Sn wires have stronger differences between mechanical properties of the wire components than Nb-Ti wires. Hence Nb_3Sn wires cannot be deformed to the same extent as Nb-Ti wires during cabling and are generally more prone to cabling degradation. Cabling studies of RRP wires [1], [4] have shown that the compaction of the Rutherford cable, in particular at the minor edge of keystone cables, should be carefully controlled to minimize strand degradation. Excessive deformation at the cable edges was observed to cause severe deformation of sub-elements and rupture of their diffusion barriers. Two consequences are then important: (1) Sn can freely leak into the stabilizer; and (2) Nb_3Sn regions of adjacent sub-elements can merge. The former leads to lowering the *RRR* of Cu and loss of thermal conductivity. The latter can possibly lead to the sintering of sub-elements and an approximate doubling of the effective filament diameter, D_{eff}. Both these effects reduce J_s strongly in the vicinity of the cable edge, possibly preventing recovery from quenches induced by flux jumps at that location. Indeed, extracted strands from overly compacted cables showed reduced J_c and J_s.

To simulate strand deformation at the cable edge, round strands can be passed through a rolling mill prior to the reaction heat treatment. The effect of deformation on the properties of the strands can then be evaluated to set limits for cabling parameters. Barzi *et al.* [5] coordinated extensive light microcopy analyses with rolling of RRP and powder-in-tube wires to reveal how the kinds of damage discussed for cables in the paragraph above can be reproduced by rolling experi-

Manuscript received August 28, 2007. This work supported by the U.S. Department of Energy under Contract No. DE-AC02-98CH10886.

A.K. Ghosh is with the Magnet Division, Brookhaven National Laboratory, Upton, NY 11973, USA (corresponding author, phone: 631-344-3974; fax: 631-344-2190; e-mail: aghosh@bnl.gov).

L. D. Cooley was with Brookhaven National Laboratory, and is now with Fermi National Accelerator Laboratory, Batavia, IL 60510, USA (e-mail: ldcooley@fnal.gov).

D. R. Dietderich and L. Sun are with Lawrence Berkeley National Laboratory, Berkeley, CA 94720 USA (e-mail: drdietderich@lbl.gov).

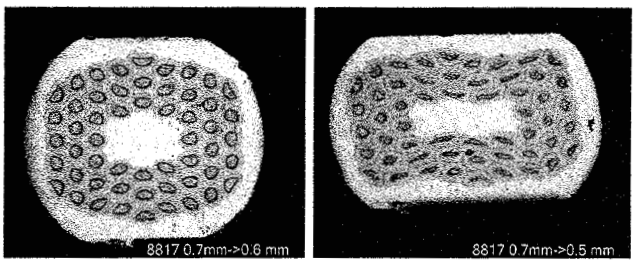

a. b.

Fig. 1. Strand cross-section of RRP-8817 rolled to 0.6 mm (a) and 0.5 mm (b).

ments. Their preliminary experiment concluded that the primary effect of deformation was an increased tendency for sub-element merging and a concomitant reduction of stability due to higher magnetization. However, the particular changes in critical current, magnetization, and *RRR* were not explored in detail.

In this paper we report on critical current, low field stability, *RRR* and the low field magnetization of RRP wires taken from three different billets. For all billets, round wires at 0.7 mm diameter were compared to strands rolled to 0.6, 0.55, 0.5, and 0.45 mm thickness. Strands from $(Nb\text{-}Ta)_3Sn$ billet 8817 consist of 54 sub-elements with a non-Cu fraction of 0.53, and were taken from LARP inventory. Two $(Nb\text{-}Ti)_3Sn$ billets 9415 and 9416 are also compared [6], taken from the US Conductor Development Program (CDP) [7]. It is important to note that these billets were restacked with material from the same sub-element billet. Billet 9415 contains 54 sub-elements with a non-Cu fraction of 0.53, and is thus very similar to billet 8817 except for the change in alloying element. Billet 9416 contains 108 sub-elements with a non-Cu fraction of 0.49. At 0.7 mm wire diameter, the average sub-element diameter for 9415 is 70 μm while that of 9416 is 50 μm, and correspondingly the Nb diffusion barrier in 9415 is thicker than in 9416.

II. MEASUREMENTS AND PROCEDURES

A. Rolling and Heat Treatment

Billet 8817 wires were deformed by OST using a rolling mill. Wires from billets 9415 and 9416 were deformed at Brookhaven National Laboratory (BNL) by pulling through a Turkshead. All strand samples were reacted in high vacuum on stainless steel barrels and then transferred to Ti-6Al-4V alloy test barrels. Wires from 8817 were reacted at 210 °C, 400 °C, and 640 °C for 48 h at each stage. Wires from 9415 and 9416 were reacted at 210 °C, 400 °C, and 650 °C for 48 h at each stage. For the rolled strands, we define the deformation ("rolling") strain ε_{roll} as $(d\text{-}t)/d$, where t is the minor rolled strand dimension (called "thickness" everywhere else in this paper) and d is the round wire diameter.

B. Wire I_c and Magnetization Measurements

The critical current, I_c, at 4.2 K was measured at BNL as a function of field as described earlier [8]. Voltage-current (*V-I*) data were acquired in 0.5 T intervals from 8 T to the 11.5 T limit of our magnet to determine J_c (criterion: 10^{-14} Ω-m). This was followed by the acquisition of voltage-field (*V-H*) data from 0 to 4 T to determine J_s. The product $J_c^{0.5}H^{0.25}$ produced data that could be fit by a line with a high degree of accuracy, and this fit was used to make $J_c(H)$ extrapolations to the 12 T conductor benchmark field. No self-field correction was applied to the data. In most cases the field was applied parallel to the broad face of the rolled strand. In some instances, the rolled strand was reacted in an orientation such that the field could be applied perpendicular to the broad face. These are indicated as Par and Perp respectively.

Magnetization measurements were conducted in a commercial SQUID magnetometer at 4.5 K between –3 to +5 T. Short pieces of the strands, approximately 7 mm long and 15 to 20 mg mass, were mounted on nonmagnetic holders such that the field was perpendicular to the strand axis. Here also, Par and Perp refer to the orientation of the rolled strand's broad face to the applied field.

III. RESULTS AND DISCUSSION

A. RRP Billet 8817

This wire is similar to that which has been used to fabricate 20-strand rectangular and 27-strand keystone cables for the LARP program [1]. Examination of these LARP cables in cross-section (done elsewhere) showed that the typical deformation strain is ~0.18 at the minor edges. The minor edge compaction of the keystone cable is nominally 94%. Fig. 1 shows the cross-sections of strands rolled to 0.6 mm (ε_{roll} = 0.14) and 0.5 mm (ε_{roll} = 0.28). Although the sub-elements at 0.6 mm show minimal deformation, some at 0.5 mm show fairly severe distortion. Examinations at higher magnification (not shown) were consistent with [5], i.e. they revealed thin and ruptured barriers and encroachment of sub-element regions into adjacent sub-elements.

Fig. 2 shows the change in strand J_c normalized to the round-wire J_{c0} as ε_{roll} is increased. J_c degradation sets in at ε_{roll}

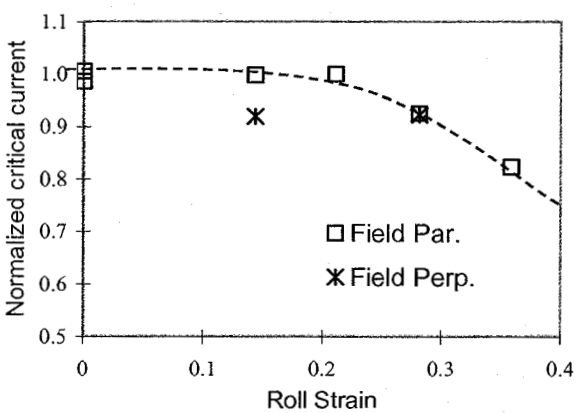

Fig. 2. Plot of J_c (12 T, 4.2K) normalized to the J_{c0} for the round strand as a function of roll strain for samples in field parallel and perpendicular to the broad face of the rolled strand. J_{c0} = 2750 A/mm^2

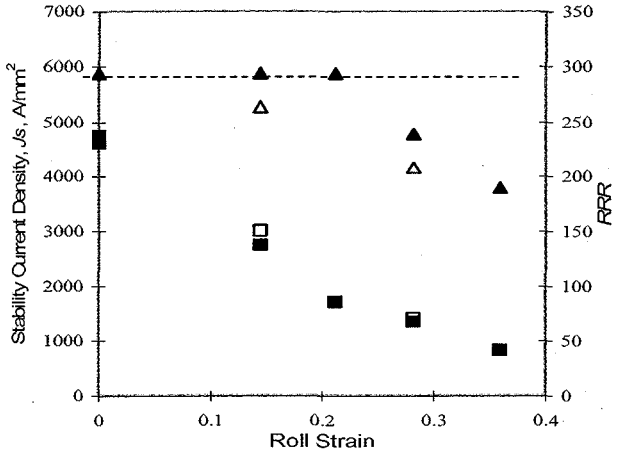

Fig. 3. Plot of J_s (▲,△) and *RRR* (■,□) as a function of ε_{roll}. The closed symbols denote parallel field, and open symbols denote perpendicular field. The dashed line indicates the highest value of J_s that can be measured.

≈ 0.15. The degradation trend passing through $\varepsilon_{roll} = 0.18$ is also consistent with the observed 5% J_c loss for extracted strands from LARP keystone cables [9]. The lack of a clear trend for the Perp measurements is likely due to the increased measurement error because the strand does not seat properly in the groove, and the low number of samples tested.

The effect of deformation on J_s and *RRR* are shown in Fig. 3. The changes in *RRR* are quite striking, given that identical final reactions were applied to the wires. *RRR* is apparently quite sensitive to ε_{roll}. This is plausible, given that there are dramatic changes in the pathways for Sn diffusion into the copper stabilizer. Constant-current stability measurements are limited to a maximum of 1200 A, which corresponds to J_s = 5900 A·mm^{-2} as denoted by the horizontal dashed line. As has been observed for round strands [9], J_s drops into the measurement range when *RRR* decreases below about 100, although here it always remains above 3000 A·mm^{-2}. Also, J_s in perpendicular field is lower than J_s in parallel field, which can be attributed to a higher Perp vs. Par magnetization. However, these differences are not that strong, leading to the conclusion that the drop in *RRR* is the stronger factor driving the reduction in J_s.

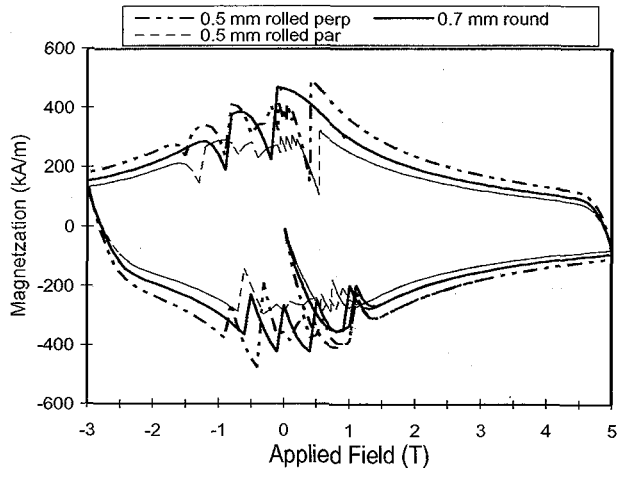

Fig. 4. A plot of magnetization at 4.5 K versus field of round and rolled wires from 8817.

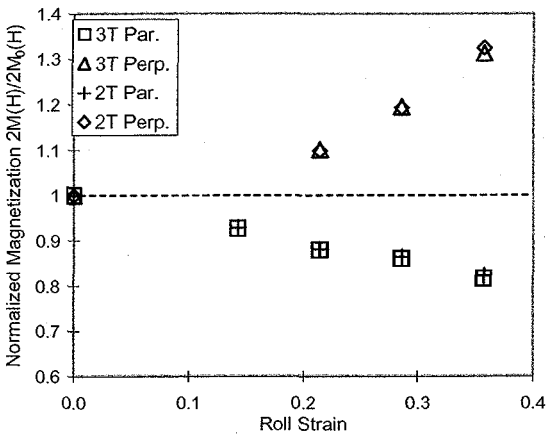

Fig. 5. A plot of the normalized magnetization width $2M$ at 2 T and 3 T versus roll strain Width for the rolled strands is normalized to the width $2M_0$ for the round 0.7 mm strand.

Magnetization measurements were taken at 4.5 K on the rolled strands to investigate changes due to sub-element merging and sintering. In Fig. 4, data for the round strand and the 0.5 mm thick strand are shown, with field H orientation denoted for the latter. Clearly, the 0.5 mm H-par magnetization is less than that of the round strand, whereas the H-perp magnetization is larger than that of the round strand. These changes, however, are not factor-of-2 variations that might be expected if 2 sub-elements merge. They can be qualitatively understood as a geometric effect that arises from the sub-elements being more rectangular when rolled rather than round. If the sub-elements are approximated as elliptical in cross-section with the large axis a and small axis b, then in field parallel to a, the magnetization is reduced by $\sim (b/a)^{1/2}$. In perpendicular field it is increased by $\sim (a/b)^{1/2}$. The observed changes as a function of roll strain (shown in Fig. 5) are less than these simple approximations because not all sub-elements are deformed uniformly into an elliptical shape. Also, the magnetization samples tested are significantly shorter than the twist pitch of the strands, preventing large loops due to periodic connections along the wire length from affecting the data. Nonetheless, the fact that the magnetization changes are consistent with the simple geometry changes indicates that effects of sub-element merging and sintering are not strong.

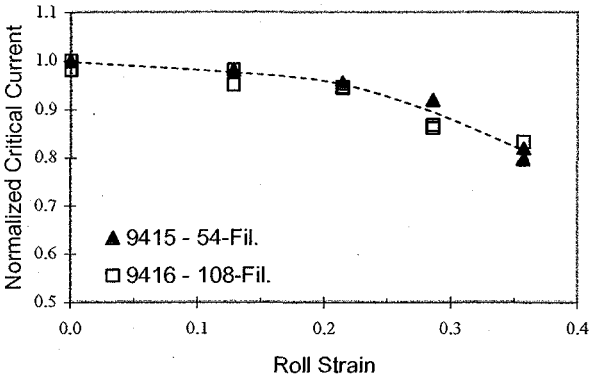

Fig. 6. Plot of J_c (12T) normalized to the J_{c0} (12T) of the round strand.

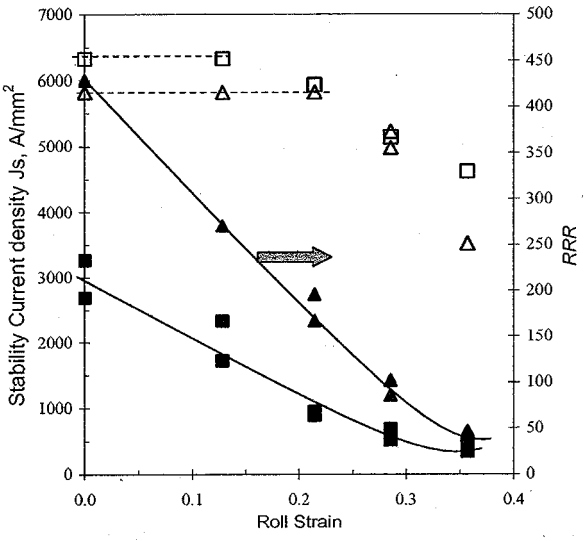

Fig. 7. Plot of J_s (open symbol) and RRR (closed symbol) for 9415 (△, ▲) and 9416 (□, ■). The dashed lines indicate the maximum J_s that can be measured for each strand due to limitations of the measurement system.

B. RRP Billets 9415 (54-Fil.) and 9416 (108-Fil.)

Because both billets were fabricated using the same sub-element, the critical current density at 12 T for 0.7 mm round wires were very similar; J_{c0} (9415) = 2975 A·mm^{-2} and J_{c0} (9416) = 2969 A·mm^{-2}. Fig. 6 is a plot of J_c normalized to J_{c0} for deformed strands. Two wires were measured for each deformation stage. Both strand designs again show similar behavior and an onset of degradation in J_c at ε_{roll} ~0.2.

The effect of rolling on the stability current density and the *RRR* is shown in Fig. 7. The round 108-sub-element 9416 strand shows lower *RRR* due to Sn contamination as compared to the 54-sub-element 9415 strand. This is due to the thinner barrier in the 108-filament conductor. Although both wires suffer *RRR* degradation due to rolling, the 108-sub-element strand has higher J_s than the 54-sub-element strand even when the *RRR* is low. This is a consequence of the smaller filament diameter and the smaller magnetization for 9416, which is shown in Fig 8. Thus, the important lesson in these data is that smaller sub-elements mitigate substantially the stability losses due to cabling damage, even despite lower *RRR*.

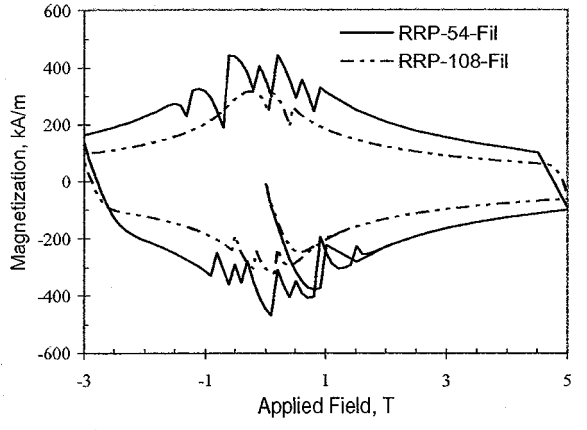

Fig. 8. Plot of magnetization versus applied field at 4.5 K of a round 0.7 mm 108 filament strand compared to a 0.7 mm 54-filament strand.

Finally, as a proof-of-principle, LBNL recently fabricated ~65 m of 27-strand 1° keystone prototype LARP cable using strand from billet 9416. Strands extracted from this cable when reacted at 650 °C for 48 h during the final stage had an average J_c(12 T) of 2940 A·mm^{-2}, a stability J_s > than 6300 A·mm^{-2} and *RRR* ≈ 216. These values are consistent with the trends in data for the deformed strand from the same billet in this study, taken at $\varepsilon_{roll} = 0.18$.

IV. Conclusion

This study found that rolled Nb_3Sn wires can be an effective way to establish performance changes due to deformation, which can be used to set parameters for cabling. It is also evident that at moderate deformation there is little loss of J_c or J_s provided barrier breakage is minimized. *RRR* is quite sensitive to degradation, which can affect stability against flux jumps at cable edges. Smaller sub-elements were effective at restoring stability even though they exhibited the lowest *RRR* of the strands studied. Future work should continue to examine the effect of deformation on other RRP strands with higher number of sub-elements and different strand architectures.

Acknowledgment

A.K.G. and L.D.C. thank the expert technical help of E. Sperry and J. D'Ambra in making the electrical measurements. The authors also thank J. Parrell, M. Field and S. Hong of OST for their assistance with rolling, provision of microscopy, and discussions.

References

[1] D. R. Dietderich, E. Barzi, A. K. Ghosh, N. L. Liggins and H. C. Higley, "Cable R&D for the LHC Accelerator Research Program", *IEEE Trans. Appl. Supercond.*, vol 17, pp. 1481-1484, 2007

[2] J. A. Parrell, Y. Zhang, R. W. Hentges, M. B. Field and S. Hong, "Nb_3Sn strand development at Oxford Superconducting Technology", *IEEE Trans. Appl. Supercond.*, vol. 13, pp. 3470-3473, 2003.

[3] A. K. Ghosh, E. A. Sperry, L. D. Cooley, A. R. Moodenbaugh, R. L. Sabatini, and J. L. Wright, "Dynamic stability threshold in high-performance internal-tin Nb_3Sn superconductors for high field magnets", *Supercond. Sci. Technol.* 18, L5 , 2005.

[4] E. Barzi *et al.*, "Performance of Nb3Sn RRP Strands and Cables Based on a 108/127 Stack Design", *IEEE Trans. Appl. Supercond.*, vol 17, pp. 2718-2721, 2007

[5] D. Turrioni, E. Barzi, M. Bossert, V. V. Kashikhin, A. Kikuchi, R. Yamada, and A. V. Zlobin, "Study of effects of deformation in Nb3Sn multi-filamentary strands", *IEEE Trans. Appl. Supercond.*, vol 17, pp. 2710-2713, 2007.

[6] M.B. Field, J.A. Parrell, Y. Zhang, M. Meinesz and S. Hong, "Internal tin Nb3Sn conductor for particle accelerator and Fusion applications", submitted to the Int. Cryogenic Materials Conf., Chattanooga, TN, 2007.

[7] R. M. Scanlan, "Conductor development for High Energy Physics-Plans and status of the U. S. Program", *IEEE Trans. Appl. Supercond*, vol. 11, p. 2150, 2001.

[8] R. Soika, L. D. Cooley, A. K. Ghosh, and A. Werner, "Fixture for short sample testing of modern high energy physics Nb_3Sn strands", *Adv. Cryo. Eng. (Materials)*, vol. 50A, pp. 67 – 74, 2004.

[9] E. Barzi, R. Bossert, S. Caspi, D. Dietderich, P. Ferracin, A. Ghosh, and D Turrioni, "RRP Nb3Sn Strand Studies for LARP", *IEEE Trans. Appl. Supercond.*, vol 17, pp. 2607-2610, 2007.